Molecular simulations on the chirality preference of single-walled carbon nanotubes upon ductile behavior under tensile stress at high temperature

Hirotoshi Deguchi[a,1], Yasutaka Yamaguchi[a,*], Kaori Hirahara[a], Yoshikazu Nakayama[a]

[a]*Department of Mechanical Engineering, Osaka University, 2-1 Yamadoka, Suita 565-0871, Japan*

Abstract

Molecular dynamics simulations were carried out on the ductile behavior of single-walled carbon nanotubes (SWNTs) under tensile stress by moving both ends at constant velocity at high temperature. The $(10, 10)$ armchair-SWNT resulted in plastic elongation through the sequential Stone-Wales (S-W) transformation, and the chirality changed keeping the two indices equal by alternately taking two dislocation directions with Burgers vectors $\vec{b} = (1, 0)$ and $(0, 1)$ instead of choosing only one of them toward zigzag-chirality with one index equal to zero. The comparison in the activation and formation energies for the two directions revealed that the torsional strain induced by the preceding S-W sequence was the main cause of this alternating choice.

Keywords: Carbon Nanotubes, Chirality, Superelastic, Dislocation

1. Introduction

Carbon nanotubes (CNTs) have attracted much attention as promising materials for use in various applications, because of their interesting features: their high aspect ratios, small size, excellent mechanical properties,

*Corresponding author

Email addresses: yamaguchi@mech.eng.osaka-u.ac.jp (Yasutaka Yamaguchi), hirahara@mech.eng.osaka-u.ac.jp (Kaori Hirahara), nakayama@mech.eng.osaka-u.ac.jp (Yoshikazu Nakayama)

[1]Presently at Denso. Corp.

and unique electronic properties. For designing CNT devices, it is crucial to understand the mechanical response of CNTs to deformation and strain.

Under tensile strain in the axial direction at a low temperature, single walled CNTs (SWNTs) would be broken theoretically with about 20 % [1].However, recent report showed that SWNTs had extreme ductility at a high temperature above 2000 °C, where the SWNT was elongated more than 280 % before the breakage [2, 3]. Regarding this ductile behavior, Yakobson et al.[4, 5] proposed a mechanism that systematic bond rearrangement called the Stone-Wales (S-W) transformation [6] displayed in Fig. 1(a) was activated under tensile stress at high temperature, and sequential propagation of S-W transformations along the helical direction would lead to the decrease of tube radius. This 5-7-7-5 defect propagation is also mentioned in a tight-binding molecular dynamics study [7].

As shown in Fig. 1(b), the network configuration consisting only of hexagonal rings is basically kept except at the forefront of the propagation with this S-W sequence, i.e. dislocation line. In this example the initial chirality, or chiral index (m, m) of an armchair-SWNT changes to $(m, m-1)$ due to the dislocation with Burgers vector $\vec{b} = (0, 1)$ while of course one with $\vec{b} = (1, 0)$ can equivalently take place in an armchair-SWNT as the first event which leads to the post chirality of $(m - 1, m)$. On the other hand, in the case of helical-SWNT with $(m, n(< m))$ chirality under tensile stress, the dislocation with $\vec{b} = (0, 1)$ is energetically preferable to the other alternative with $\vec{b} = (1, 0)$, and the post chirality after the dislocation becomes $(m, n - 1)$.

Yakobson et al.[5] explained that this preference causes the dislocation with $\vec{b} = (0, 1)$ leading to $(m, n-2)$ chirality as the second S-W sequence, and this continued until the chirality becomes $(m, 0)$ of zigzag-SWNT, because the dislocation to reduce the smaller chiral index component was always energetically advantageous. After reaching zigzag-SWNT, it would result in breakage because no dislocation path to reduce the tensile stress exists there. In addition, the second S-W sequence following the first chirality change from (m, m) to $(m, m - 1)$ in the example in Fig. 1 should be with $\vec{b} = (0, 1)$ to form $(m, m - 2)$ because of the same reason, and this process continues up to the final chirality of $(m, 0)$ as well. Hence, they claimed that the final structure was basically zigzag-SWNT with one chiral index equal to zero.

Although a more drastic structural change presumably at a higher temperature range around sublimation temperature has also been proposed including mass decrease caused by C_2 detachment [8], the mechanism with S-W

sequence seems feasible within a moderate temperature range because the S-W transformation is a structural rearrangement with the least activation energy both cutting and creating only two bonds, respectively.

Nevertheless, it is still unclear whether the preference considered in the model to choose dislocation leading to zigzag-chirality really holds also for the second and further ones. In this work, molecular dynamics (MD) simulations using classical empirical potential are performed on the ductile behavior of SWNTs under tensile stress, where SWNTs with finite length are subject to tensile load with at constant velocity at both ends. The temporal change of the structure was investigated in detail including the effect of chirality and temperature as well as static transition energy analysis for the S-W sequence.

2. Method

The interaction among carbon atoms were described by the second-REBO potential proposed by Brenner et al. [9], where the compensation term b_{ij}^{π} in the original reference was omitted here. Armchair-, zigzag- and chiral-SWNTs of a length about 7 nm with chiral index $(m, n) = (10, 10)$, $(17, 0)$, and (13.7), respectively were adopted as the sample SWNTs. In the MD simulations, tensile stress was imposed on the SWNTs by moving the three layers at both ends of the SWNTs at a constant velocity $\pm u_0/2$ with $u_0 = 5.0 \times 10^{-3}$ m/s for 200 nanoseconds, where the relative positions inside the three layers were fixed and no rotational moment was imposed. The vibrational temperature of the system was controlled at constant temperatures T_c ranging from 2200 to 3000 K by the velocity rescaling method. Ten calculation runs were carried out for each by giving small initial deviation in the velocities.

The nudged elastic band (NEB) method [10] was adopted as well in order to calculate the static activation energy E_a for the S-W transformation. Similar to the MD simulation, carbon atoms in three layers at both ends of the SWNT were fixed in this static analysis. Fifteen image phases were inserted between the pre- and post-phases at fully relaxed molecular orientations at local mimima, and a linear spring with a spring constant of 1.0×10^4 N/m was appended between each identical atom pair in neighboring phases. The formation energy E_f was simply defined as the energy difference between post- and pre-phases at local mimima.

Due to the computational limitation the strain rate about 7×10^5, which is much higher than the experimental condition, is adopted in order to accelerate the simulation. Accordingly the temperature range between 2200

and 3000 K is set higher than the experimental condition so that the tensile stress can be smoothly released through systematic S-W sequence. Through the NEB calculation, the minimum activation energy of the first S-W transformation in $(10, 10)$ perfect SWNT is estimated about 7.5 eV without strain and about 6 eV with 3 % strain.

3. Results and discussion

Figure 2 shows the simulation snapshots of $(10, 10)$ armchair-SWNT at 200 ns for control temperatures T_c of 2400 and 3000 K. A bond line is depicted between pair of atoms with its distance shorter than 1.8 Å and bold lines denote interatomic bonds which form 5- and 7-membered rings. The SWNT simply resulted in fracture at lower control temperatures under 2400 K. Ductile behavior appeared at higher temperatures, and especially at $T_c = 3000$ K, helical propagation of 5-7 defects due to S-W sequence was often observed as indicated with two arrows at 50 ns in Fig. 2 (b) so that the tensile stress could be released with holding the ordered structure consisting only of hexagonal network.

It should also be noted that threshold temperature leading to fracture or ductile behavior should be determined by the balance between the strain rate and activation energy of the S-W defect as mentioned above, and therefore the temperature would be reduced with much lower strain rate applied in experiment.

Five examples of chirality change in armchair-SWNT at 3000 K out of ten simulation runs are illustrated in Fig. 3. The initial chirality is $(m, n) = (10, 10)$, and chirality histories are depicted here around the local area where the tube radius is the smallest at 200 ns. All showed ductile elongation with helical propagations of 5-7 defects, and the radius of the armchair-SWNT decreased with keeping the two chiral indices m and n equal, i.e. keeping the armchair-chirality by alternately choosing the two dislocation paths with Burgers vectors $\vec{b} = (1, 0)$ and $(0, 1)$. These results are obviously contradictory to those expected from the above-mentioned model that even an armchair-SWNT goes to zigzag-chirality with reducing only one of the chiral indices of m and n until zero by choosing only one dislocation path with identical Burgers vector after the first alternative choice.

In order to trace the dislocation paths, the network map around the plastically elongated region is displayed in Fig. 4 for armchair- and chiral-SWNTs with initial chiral index $(m, n) = (10, 10)$ and $(13, 7)$, respectively

after ductile elongation at 200 ns for control temperature $T_c = 3000$ K. Here the network map is unfolded along the radial direction and therefore, the top and bottom sides are periodically connected. The bold white lines denote bond lines whose angle to the tube axis has largely been changed from the initial angle, and this should extract bonds which have experienced the S-W transformation as shown in Fig. 1. Two directions with Burgers vectors $\vec{b} = (1, 0)$ and $(0, 1)$ for the S-W sequence were clearly observed for armchair-SWNT in Fig. 4 (a). It should also be noted that the S-W sequence did not seem to infinitely propagate but stopped at a finite length. On the other hand, only one direction with $\vec{b} = (0, 1)$, which reduced the second chiral index n, was seen for chiral-SWNT in Fig. 4 (b), thus the chirality went toward zigzag one with $n = 0$. The $(17, 0)$ zigzag-SWNTs did not show any ductile behavior and resulted in simple breakage around the center in all simulation runs. This is attributed to the fact that no dislocation path would reduce the tensile stress.

A question arises here why an armchair-SWNT keeps the armchair chirality with two chiral indices m and n equal upon ductile elongation, although an SWNT with uneven chirality $(m, n(\neq m))$, which is achieved even in an armchair-SWNT after the first dislocation, should energetically choose a dislocation path to reduce the smaller index. This seems to be closely related to the above-mentioned fact that the propagation of S-W sequence stopped at a finite length in Fig. 4.

Figure 5 shows the formation energy E_f upon each S-W transformation with the Burgers vector $\vec{b} = (1, 0)$ for the $(10, 10)$ armchair-SWNT with an initial tensile strain of 3 %. The alternative dislocations with $\vec{b} = (0, 1)$ results in the same in this case. Although the formation energy for initial two steps were positive, it stayed negative up to the 21st step showing that the SWNT was stabilized through the reduction of tensile stress by the propagation of the S-W sequence until this step. A snapshot after 21 S-W sequential transformations is also displayed in Fig. 5, where the 5- and 7-membered rings at the dislocation forefronts are shaded. It is clear that the SWNT is highly twisted, and due to the increase of this torsional strain, the formation energy then switched back to positive again upon the further S-W sequence although the tensile strain is reduced. The stopping of the S-W propagation in Fig. 4 can also be attributed to this re-increase of the formation energy.

A question arises again why torsional stress is imposed to the SWNT due to the S-W sequence. A cartoon image of an armchair-SWNT after the

S-W transformation sequence with the Burgers vector $\vec{b} = (1, 0)$ is illstrated in Fig. 6. It is clear from this that the SWNT can be elongated with the S-W transformation sequence while it is also accompanied with torsional motion around the tube axis. Thus in case the tube end is fixed, inevitable torsional stress works on the SWNT, and it should also be true for a longer SWNT because of the torsional rigidity. Although the release of tensile strain and the accumulation of torsional strain are in trade-off relation while the induced torsional strain per tensile strain release becomes larger as the angle between the tube axis and Burgers vector becomes larger as expected from Fig. 6. Therefore, the torsional strain on the elongated $(13, 7)$ chiral-SWNT in Fig. 4, which has smaller angle between the tube axis and Burgers vector, is still not large enough to activate S-W sequence with $\vec{b} = (1, 0)$ to release the torsion.

Considering that the propagation of S-W sequence stops with a finite length, the preference to choose $\vec{b} = (1, 0)$ or $(1, 0)$ as the following dislocation direction should depend on the pre-existing S-W sequence. In order to examine this effect, the activation and formation energies E_a and E_f of S-W transformations with Burgers vectors $\vec{b} = (0, 1)$ and $(1, 0)$ were calculated for a $(10, 10)$ armchair-SWNT with preceding S-W sequence up to 15 steps with $\vec{b} = (0, 1)$ as in Fig. 7. The initial tensile strain is set to 3 %, and the energies for a $(10, 9)$ perfect chiral-SWNT without defect, a consequence of $(10, 10)$ SWNT after dislocation with $\vec{b} = (0, 1)$ without torsion, is also displayed for comparison. Note that the 5-7 defects after 15 S-W transformations are still far from the fixed boundary here. In addition, the first S-W transformation is simply rotating one bond for both Burgers vectors and hence the values are the same. The S-W sequence with $\vec{b} = (0, 1)$ for the $(10, 9)$ perfect SWNT gave lower values of E_a and E_f than with $\vec{b} = (1, 0)$ as expected in Yakobson's model, indicating that the former would be chosen as the first dislocation. On the contrary, the S-W sequence with $\vec{b} = (1, 0)$ resulted in lower activation and formation energies for the $(10, 10)$ SWNT with preceding dislocation, and therefore, this should be a preferable S-W sequence there. The alternating choice seen in Fig. 3 is ascribed to this fact that a dislocation leading to further uneven chiral indices in an armchair-SWNT would give rise to higher activation and formation energies. This preference should hold except in the case that the torsional strain brought by the dislocation is fully relaxed at the end boundary, while both sides of a sample SWNT under tensile load is often tightly fixed in experiments [2, 3]. This tendensity of alternately

taking two dislocation directions is also indicated in our recent experiment using SWNT near armchair-chirality [11].

4. Concluding remarks

Molecular dynamics simulations were carried out on the ductile behavior of SWNTs under tensile stress by moving both ends at constant velocity at high temperature. The $(10, 10)$ armchair-SWNT resulted in plastic elongation through the sequential S-W transformation, and the chirality changed keeping the two indices equal by alternately taking two dislocation directions with Burgers vectors $\vec{b} = (1, 0)$ and $(0, 1)$ instead of choosing only one of them toward zigzag-chirality. The comparison in the activation and formation energies for the two directions revealed that the torsional strain induced by the preceding S-W sequence was the main cause of this alternating choice.

Acknowledgments

Y.Nakayama express his thanks to the Ministry of Education, Science and Culture of Japan for support by a Grant-in-Aid for Scientific Research on the Priority Area "Carbon Nanotube Nano-Electronics".

References

[1] H. Mori, Y. Hirai, S. Ogata, S. Akita, Y. Nakayama, Chirality dependence of mechanical properties of single-walled carbon nanotubes under axial tensile strain, Jpn. J. Appl. Phys. 44 (2005) L1307–L1309.

[2] J. Y. Huang, S. Chen, Z. Q. Wang, K. Kempa, Y. M. Wang, S. H. Jo, G. Chen, M. S. Dresselhaus, Z. F. Ren, Superplastic carbon nanotubes, Nature 439 (2006) 281–281.

[3] J. Y. Huang, S. Chen, Z. F. Ren, Z. Wang, K. Kempa, M. J. Naughton, G. Chen, M. S. Dresselhaus, Enhanced ductile behavior of tensile-elongated individual double-walled and triple-walled carbon nanotubes at high temperatures, Phys. Rev. Lett. 98 (2007) 185501/1–4.

[4] B. Yakobson, Mechanical relaxation and 'intra-molecular plasticity' in carbon nanotubes, Appl. Phys. Lett. 72 (1998) 918–920.

[5] M. B. Nardelli, B. I. Yakobson, J. Bernholc, Brittle and ductile behavior in carbon nanotubes, Phys. Rev. Lett. 81 (1998) 4656–4659.

[6] A. Stone, D. Wales, Theoretical study of icosahedral c60 and some related species, Chem. Phys. Lett. 128 (1986) 501–503.

[7] D. B. Zhang, R. D. James, T. Dumitricâ, Dislocation onset and nearly axial glide in carbon nanotubes under torsion, J. Chem. Phys. 130 (2009) 071101/1–4.

[8] F. Ding, K. Jiao, M. Wu, B. I. Yakobson, Pseudoclimb and dislocation dynamics in superplastic nanotubes, Phys. Rev. Lett. 98 (2007) 075503/1–4.

[9] D. W. Brenner, O. A. Shenderova, J. A. Harrison, S. J. Stuart, A second-generation reactive empirical bond-order (rebo) potential energy expression for hydrocarbons, J. Phys.: Condens. Matter 14 (2002) 783–802.

[10] G. Henkelman, H. Jónsson, Improved tangent estimate in the nudged elastic band method for finding minimum energy paths and saddle points, J. Chem. Phys. 113 (2000) 9978–9985.

[11] K. Hirahara, K. Inose, Y. Nakayama, Determination of the chiralities of isolated carbon nanotubes during superplastic elongation process, Appl. Phys. Lett. 97 (2010) 051905/1–3.

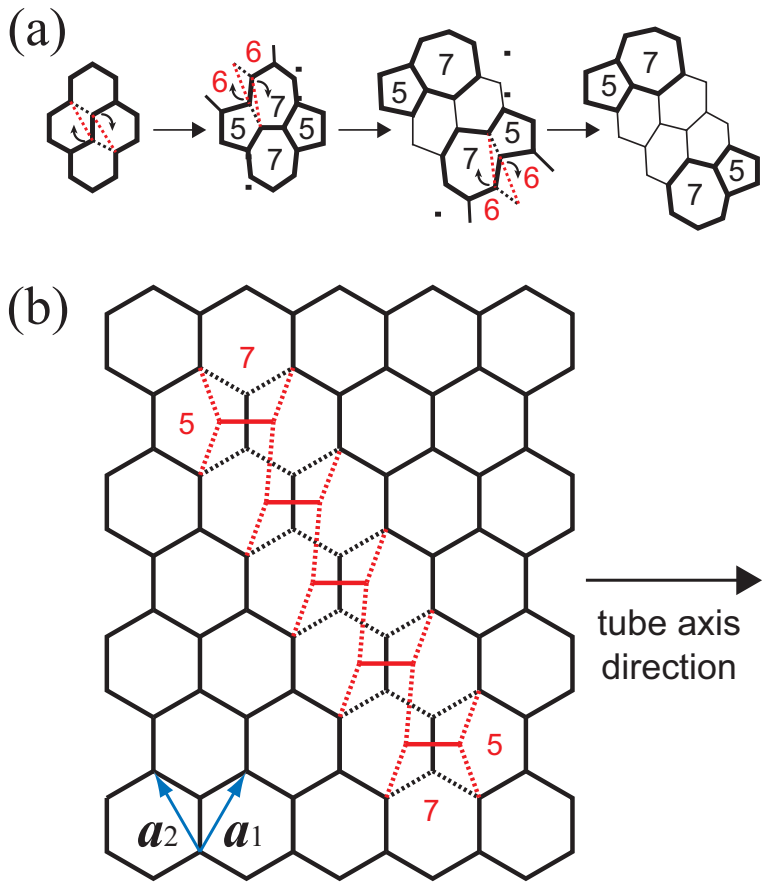

Figure 1: Bond rearrangement via the sequential Stone-Wales (S-W) transformation. (a) Detailed mechanism up to three sequential S-W transformation, where the inter-atomic bond at circular arrows flips by 90 degrees upon network change with both creating (red dotted) and cutting (black dotted) two bonds per bond-flip. (b) Change of bond network in armchair-SWNT with an initial chirality of (m, m) after nine sequential bond flips with a Burgers vector $\vec{b} = (0, 1)$. The expansion plan unfolded parallel to the tube axis is illustrated, and initial configuration is shown in black lines. Five vertical black solid bonds perpendicular to red solid bonds are apparently rotated by 90 degrees. Red dotted bonds are newly formed while black dotted bonds are cut through the S-W sequence. Pairs of five- and seven-membered rings remain only at the forefront of the S-W sequence, and the post chirality is $(m, m-1)$ in this case with $\vec{b} = (0, 1)$.

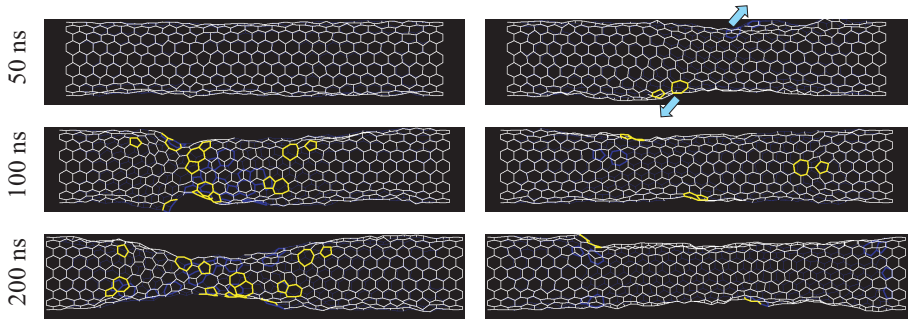

(a) T_c = 2400 K (b) T_c = 3000 K

Figure 2: Simulation snapshots of $(10, 10)$ armchair-SWNT up to 200 ns for control temperatures T_c of 2400 and 3000 K with a tensile rate v_{tens} of 2.5×10^{-3} m/s. A bond line is depicted between pair of atoms with its distance shorter than 1.8 Å and bold lines denote interatomic bonds which form 5- and 7-membered rings. Helical propagation of 5-7 defects due to S-W sequence is seen at 50 ns for T_c=3000 K as indicated with two arrows.

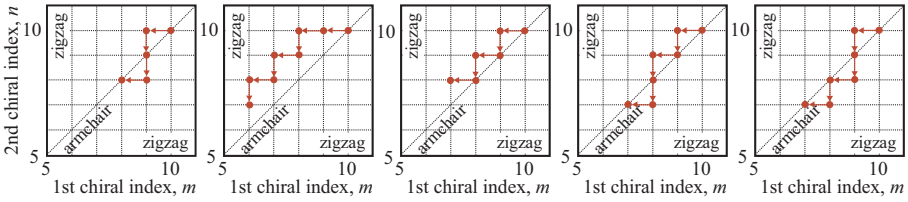

Figure 3: Examples of chirality change in armchair-SWNT at 3000 K out of ten simulation runs. The initial chirality is $(m, n) = (10, 10)$, and chirality histories are depicted here at the local area where the tube radius is the smallest at 200 ns.

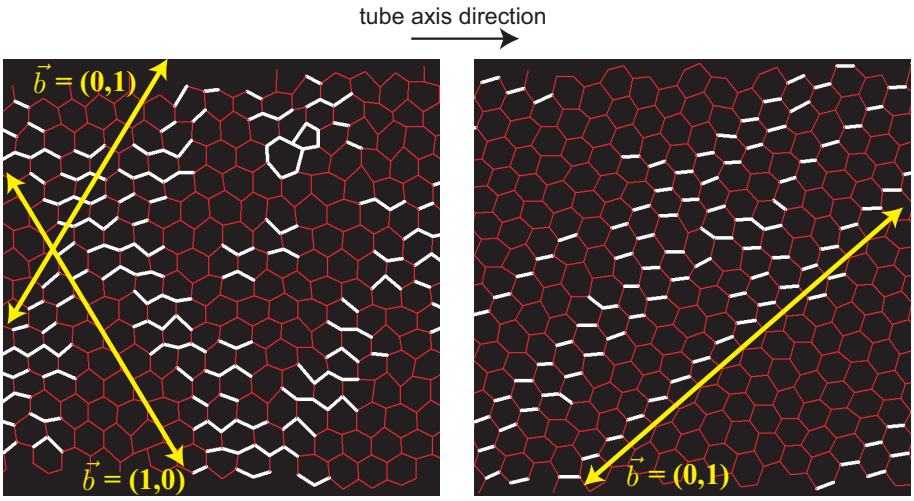

(a) (10,10) armchair-SWNT (b) (13,7) chiral-SWNT

Figure 4: Network map around the plastically elongated region for armchair- and chiral-SWNTs with initial chiral index $(m, n) = (10, 10)$ and $(13, 7)$, respectively after ductile elongation at 200 ns for control temperature $T_c = 3000$ K. The network map is unfolded parallel to the tube axis. The bold white lines denote bond lines whose angle to the tube axis has largely been changed from the initial angle.

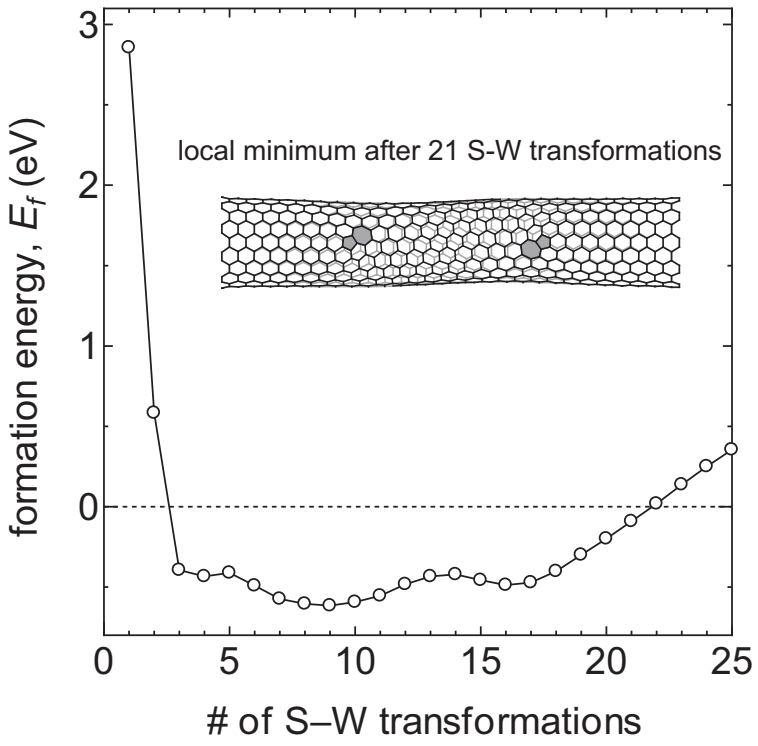

Figure 5: Formation energy upon each S-W transformation with the Burgers vector $\vec{b} = (1, 0)$ for the $(10, 10)$ armchair-SWNT with an initial tensile strain of 3 %. Snapshot after 21 S-W sequential transformations is also displayed where the 5- and 7-membered rings at the dislocation forefronts are shaded.

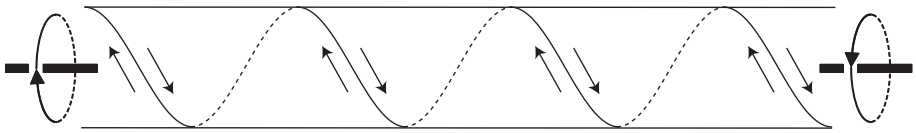

Figure 6: A cartoon image of induced twist on an armchair-SWNT after S-W transformation with the Burgers vector $\vec{b} = (1, 0)$.

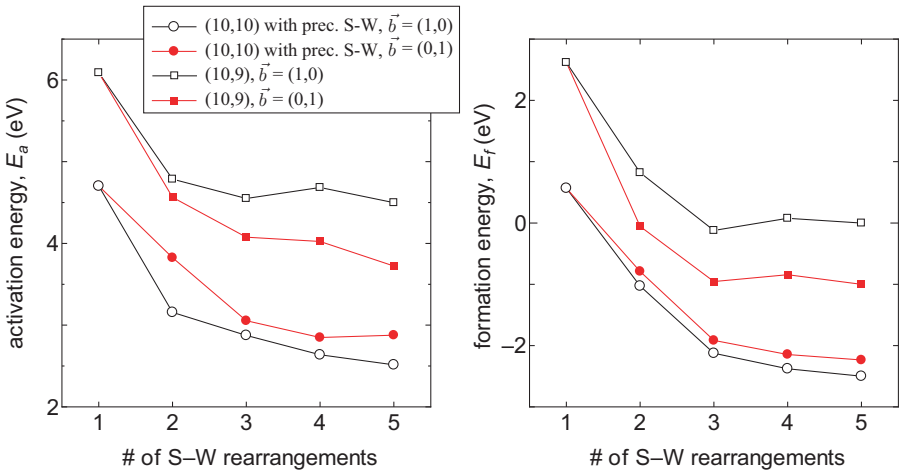

Figure 7: Activation and formation energies E_a and E_f of S-W transformations with Burgers vectors $\vec{b} = (0, 1)$ and $(1, 0)$ for a $(10, 10)$ armchair-SWNT with preceding S-W sequence up to 15 steps with $\vec{b} = (0, 1)$. The initial tensile strain is 3 %. The energies for a $(10, 9)$ perfect chiral-SWNT without defect is also displayed for comparison.